Ann Nucl Med (2015) 29:325–335
DOI 10.1007/s12149-015-0948-8

ORIGINAL ARTICLE

Radiosynthesis and in vivo evaluation of two imidazopyridineacetamides, [^{11}C]CB184 and [^{11}C]CB190, as a PET tracer for 18 kDa translocator protein: direct comparison with [^{11}C](*R*)-PK11195

Kentaro Hatano · Katsuhiko Sekimata · Takashi Yamada · Junichiro Abe · Kengo Ito · Mikako Ogawa · Yasuhiro Magata · Jun Toyohara · Kiichi Ishiwata · Giovanni Biggio · Mariangela Serra · Valentino Laquintana · Nunzio Denora · Andrea Latrofa · Giuseppe Trapani · Gaetano Liso · Hiromi Suzuki · Makoto Sawada · Masahiko Nomura · Hiroshi Toyama

Received: 27 June 2014 / Accepted: 14 January 2015 / Published online: 24 January 2015

Abstract
Objective We report synthesis of two carbon-11 labeled imidazopyridines TSPO ligands, [^{11}C]CB184 and [^{11}C]CB190, for PET imaging of inflammatory process along with neurodegeneration, ischemia or brain tumor. Biodistribution of these compounds was compared with that of [^{11}C]CB148 and [^{11}C]*(R)*-PK11195.
Methods Both [^{11}C]CB184 and [^{11}C]CB190 having ^{11}C-methoxyl group on an aromatic ring were readily prepared using [^{11}C]methyl triflate. Biodistribution and metabolism of the compounds were examined with normal mice. An animal PET study using 6-hydroxydopamine treated rats as a model of neurodegeneration was pursued for proper estimation of feasibility of the radioligands to determine neuroinflammation process.
Results [^{11}C]CB184 and [^{11}C]CB190 were obtained via *O*-methylation of corresponding desmethyl precursor using [^{11}C]methyl triflate in radiochemical yield of 73 % (decay-corrected). In vivo validation as a TSPO radioligand was carried out using normal mice and lesioned rats. In mice, [^{11}C]CB184 showed more uptake and specific binding than [^{11}C]CB190. Metabolism studies showed that 36 % and 25 % of radioactivity in plasma remained unchanged 30 min after intravenous injection of [^{11}C]CB184 and [^{11}C]CB190, respectively. In the PET study using rats, lesioned side of the brain showed significantly higher uptake than contralateral side after i.v. injection of either [^{11}C]CB184 or [^{11}C](*R*)-PK11195. Indirect Logan plot analysis revealed distribution volume ratio (DVR) between the two sides which might indicate lesion-related elevation of TSPO binding. The DVR was 1.15 ± 0.10 for [^{11}C](*R*)-PK11195 and was 1.15 ± 0.09 for [^{11}C]CB184.
Conclusion The sensitivity to detect neuroinflammation activity was similar for [^{11}C]CB184 and [^{11}C](*R*)-PK11195.

K. Hatano · K. Sekimata · T. Yamada · J. Abe · K. Ito
Department of Clinical and Experimental Neuroimaging, Center for Development of Advanced Medicine for Dementia, National Center for Geriatrics and Gerontology, Obu, Aichi 474-8522, Japan

Present Address:
K. Hatano (✉)
Faculty of Medicine, University of Tsukuba, Tsukuba 305-8575, Japan
e-mail: hatanok@md.tsukuba.ac.jp

M. Ogawa · Y. Magata
Medical Photonics Research Center, Hamamatsu University School of Medicine, Hamamatsu, Shizuoka 431-3192, Japan

J. Toyohara · K. Ishiwata
Research Team for Neuroimaging, Tokyo Metropolitan Institute of Gerontology, Tokyo 173-0015, Japan

G. Biggio · M. Serra
Department of Experimental Biology, University of Cagliari, 09100 Cagliari, Italy

V. Laquintana · N. Denora · A. Latrofa · G. Trapani · G. Liso
Pharmaco-Chemistry Department, University of Bari, Via Orabona 4, 70125 Bari, Italy

H. Suzuki · M. Sawada
Research Institute of Environmental Medicine, Nagoya University, Nagoya, Aichi 464-8601, Japan

M. Nomura · H. Toyama
Department of Radiology, Fujita Health University, Toyoake, Aichi 470-1192, Japan

Keywords Positron emission tomography · TSPO · PBR · Neuroinflammation · Alzheimer's disease

Introduction

Translocator protein (18 kDa) (TSPO) formerly referred to as peripheral benzodiazepine receptor (PBR) is a transmembrane multimeric protein complex primarily located in the outer mitochondrial membrane of cells [1]. It is especially concentrated in the outer/inner mitochondrial membrane contact sites [2], where it has been suggested to form a complex with other proteins such as the voltage-dependent anion channel and the adenine nucleotide transporter [3, 4]. TSPO is involved in various cell functions including porphyrin transport, heme biosynthesis, cholesterol transport, cell proliferation, apoptosis and anion transport [reviewed in 5, 6]. In central nervous system (CNS), TSPO is considered an ideal marker molecule for microglia activation [7]. Microglia undergo changes from a resting to an activated phenotype in response to a wide variety of CNS insults such as infectious diseases, inflammation, trauma, ischemia, brain tumors and neurodegeneration [8, 9]. Accumulation of a TSPO radioligand in lesioned area of brain is believed to be related with this microglia activation, and this is a key concept of clinical imaging of degenerative disorders of brain such as Alzheimer's disease by the means of positron emission tomography (PET) and this type of radioligand [7]. Our group reported that uptake of a TSPO radioligand, [^{11}C](*R*)-PK11195 was more related to this activation than number of the microglia cells [10] and suggested unknown mechanisms underlying the facilitated uptake of a TSPO radioligand.

[^{11}C](*R*)-PK11195 was the first TSPO radioligand applied to CNS diseases involving neuroinflammation process with PET [11]. Many clinical brain imaging studies were reported [reviewed in 8], however, the high degree of nonspecific uptake of [^{11}C](*R*)-PK11195 complicates the quantification and modeling of the PET data [12–15]. This significantly limits its sensitivity in detecting brain disorders. In this consequence, numerous radioligands for TSPO have been reported (Fig. 1). Zhang first reported carbon-11 labeled phenoxyphenyl acetamide, DAA1106 [16] and its fluoroalkyl congeners [17]. Briard reported structurally related phenoxypyridinyl acetamide, [^{11}C]PBR28 [18] and later Wilson also offered its fluoroalkyl congener, [^{18}F]FEPPA [19]. Another structural category should be referred to as "heterocyclic acetamide". Kassiou and coworkers reported pyrazolopyrimidinyl acetamides, [^{11}C]DPA-713 [20] and [^{18}F]DPA-714 [21]. Another example was dihydropurinylacetamide, [^{11}C]AC-5216 contributed by Zhang et al. [22]. Mattner offered I-123 labeled imidazopyridineacetamide, [^{123}I]CLINDE, for single photon emission computed tomography imaging [23].

We also reported four compounds of this class [24]. Only compound **[^{11}C]7** in the paper which is currently renamed as [^{11}C]CB148 showed satisfactory performance as a TSPO ligand in vivo. In the present article we report another two imidazopyridines, [^{11}C]CB184 and [^{11}C]CB190, with an ^{11}C-methoxyl group on an aromatic ring (Fig. 2). Feasibility of the compounds was examined

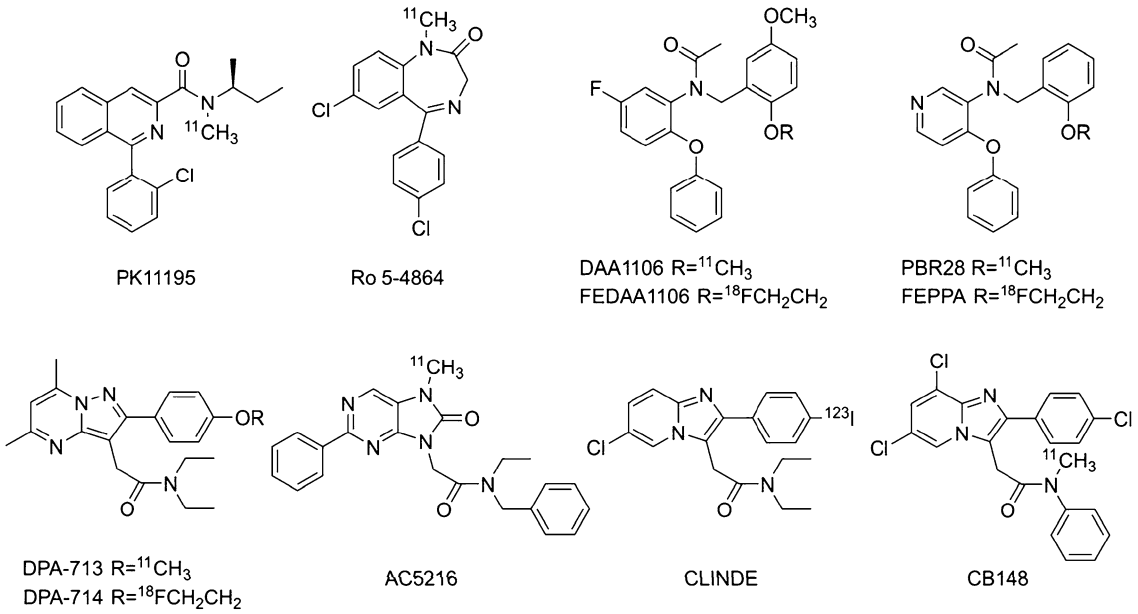

Fig. 1 Structures of TSPO radioligands

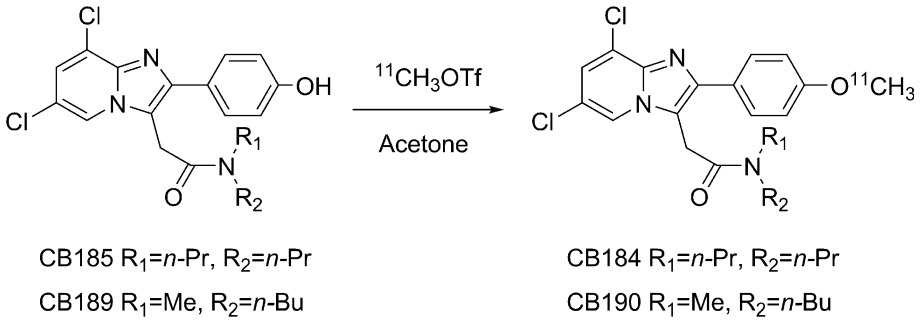

Fig. 2 Scheme of radiosynthesis

using intact mice following our previous report. In addition to this, we employed rat injury model of neurodegenerative disease. Measurement using high resolution animal PET and precise posthumous examination of the animals would reveal relevance of the methodology as well as the feasibility of the compounds in more persuasive manner, although there exist some difficulties pursuing this type of animal model study such as measurement and quantification method or appropriateness of the animal employed as human disease model. This study indicates proper direction for examining TSPO ligand performance.

Materials and methods

General

Reverse-phase high performance liquid chromatography (HPLC) was performed using LC-10A HPLC system (Shimadzu, Kyoto, Japan) accompanied by gamma ray detection using a NaI (Tl) scintillation system. An automated gamma counter with a NaI (Tl) detector (COBRA, Packard Instrument, Meriden, CT) was used to measure the radioactivity of samples from animal and partition coefficient studies. Male ddY mice and Wistar rats were supplied by Japan SLC (Hamamatsu, Japan) and Nihon Charles River (Tokyo, Japan), respectively. The present animal study was approved by the institutional committees for animal studies. Racemic PK11195 was purchased from Sigma (St. Louis, MO) and 0.1 M lithium aluminum hydride solution in tetrahydrofuran and a desmethyl derivative of (*R*)-PK11195 was purchased from ABX (Radeberg, Germany). Other chemicals were purchased from Kanto Chemicals (Tokyo, Japan) and were of the highest grade commercially available. All statistical analyses were carried out using StatView (SAS Institute Inc., Cary, NC).

Radiochemical syntheses

Unlabeled reference standard of CB184 and CB190 and their precursors, CB185 and CB189 were prepared according to previously reported method [25]. Carbon-11 was produced by $^{14}N(p, \alpha)^{11}C$ nuclear reaction using a CYPRIS HM18 cyclotron (Sumitomo Heavy Industries, Tokyo, Japan). $[^{11}C]CO_2$ thus obtained was converted to [^{11}C]methyl triflate using an automated synthesis system (CUPID C-11-BII, Sumitomo Heavy Industries, Tokyo, Japan). The obtained [^{11}C]methyl triflate was trapped in 0.3 mL acetone solution of containing 1 mg of CB185 or CB189 and 0.4 mg of NaOH (Fig. 3). The mixture was then heated at 80 °C for 3 min allowing the methylation reaction to occur. HPLC fractions containing purified [^{11}C]CB184 or [^{11}C]CB190 were collected into an evaporating vessel (HPLC conditions are summarized in Table 1). After removal of solvent, the residue was redissolved in the appropriate solvent and analyzed by reverse-phase HPLC (Table 1). The specific radioactivity of compounds was calculated by comparing the injected radioactivity with the corresponding UV peak area at 250 nm. Radiochemical synthesis of [^{11}C](*R*)-PK11195 was reported elsewhere [26].

Binding affinity and octanol/water partition coefficient

Binding affinity toward TSPO and central benzodiazepine receptor (CBR) and partition coefficient (Log *P*) were measured according to our previous report [24]. Separately, Log *P* value was calculated with CLOGP program [24].

Biodistribution in mice

A solution of [^{11}C]CB184, [^{11}C]CB190 or [^{11}C](*R*)-PK11195 in physiological saline containing 0.25 % polysorbate 80 (4 MBq/0.1 mL, 60–180 ng) was injected in male ddY mice (8–10 weeks old, 33–38 g, $n = 4$ for each group) via the tail vein. The mice were euthanized at 1, 15, 30 and 60 min after injection. Blood was removed by heart puncture using a syringe. Brain was dissected into olfactory bulb, cerebral cortex, striatum, thalamus, midbrain, cerebellum, and pons. The organs and the brain areas were weighed and the radioactivity was measured with a gamma counter. The raw counts were decay corrected to a standard

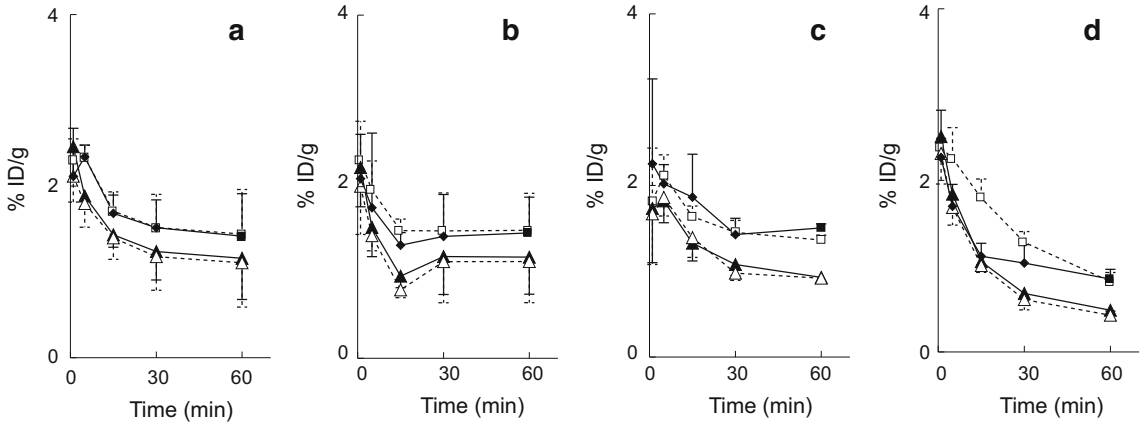

Fig. 3 Regional brain distribution; regional brain distribution of radioactivity after tail-vein injection of [^{11}C]CB184, [^{11}C]CB190, [^{11}C]CB148 and [^{11}C](*R*)-PK11195 in ddY mice is shown in **a**–**d**, respectively. Data are expressed as percentage of the injected dose per gram of tissue (%ID/g, mean and SD of four animals). *open circle* cerebellum, *filled circle* thalamus, *open triangle* cortex, *filled triangle* olfactory bulb. Data of [^{11}C]CB148 (**c**) was taken from literature [24]

Table 1 HPLC conditions

Compound	Eluent	Flow rate (mL/min)	Retention time (min)
Preparative			
CB184	Acetonitrile:H_2O (6:4)	6	9.1
CB190	Acetonitrile:H_2O (55:45)	6	10.1
Analytical			
CB185	Acetonitrile:H_2O (7:3)	1	7.8
CB190	Acetonitrile:H_2O (65:35)	1	8.0

Conditions employed for preparative and analytical HPLC are shown. Preparative HPLC was carried out using a Capcellpak C18 UG120S-5 μm column (10 mm inner diameter (i.d.) × 250 mm, Shiseido, Tokyo, Japan) and a JASCO HPLC system (JASCO, Tokyo, Japan) installed within the radiosynthesis system. Analytical HPLC was conducted using a Capcellpak C18 UG120S-5 μm column (4.8 mm i.d. × 250 mm, Shiseido, Tokyo, Japan) and a Shimadzu HPLC system (Shimadzu, Kyoto, Japan) with gamma ray detection using NaI(Tl) scintillator

time and the results were expressed as percentage of the injected does per gram of tissue (%ID/g).

Blocking studies

Mice (9–10 weeks old, 35–38 g, $n = 4$) were given via the tail vein with 0.1 mL of PK11195 in DMSO or flumazenil in physiological saline. All drugs were administered at dose of 1 mg/kg. A solution of each radioligand (prepared as above, 4 MBq/0.1 mL, 60–170 ng) was injected at 1 min after the cold drug treatment. At 30 min post-injection of the radioligand, the mice were euthanized and processed to measure %ID/g as above. Data were analyzed one-way ANOVA with Bonferroni's correction. Differences were considered significant at a p value less than 0.0167.

Metabolite studies

[^{11}C]CB184 or [^{11}C]CB190 (50–167 MBq, 0.46–1.1 μg) was intravenously injected into mice (8–9 weeks old, 36–39 g, $n = 3$ for each tracer), and 30 min later they were killed by cervical dislocation. Blood was removed by heart puncture using a heparinized syringe, and the brain was removed. After centrifugation of the blood at 7,000×g for 1 min at 4 °C the plasma of obtained, and 0.2–0.3 mL of the plasma was diluted with water up to 0.5 mL and denatured with 0.5 mL of acetonitrile in an ice-water bath. The suspension of plasma was centrifuged in the same condition and divided into soluble and precipitable fractions. The precipitate was re-suspended in 0.5 ml of acetonitrile followed by centrifugation. This procedure was repeated twice. The cerebellum (61–80 mg) was homogenized in 1 mL of a mixture of acetonitrile/water (1/1, v/v). The homogenate was treated as described above. Radioactivity in the three soluble fractions and precipitates was measured with gamma counter. In this treatment, the recovery yields in the soluble fraction were 80.3 ± 3.3 and 99.6 ± 0.1 % for plasma and brain, respectively, of mice given [^{11}C]CB184, and 96.6 ± 3.3 and 99.7 ± 0.3 % for plasma and brain, respectively, of mice given [^{11}C]CB190. The soluble fractions were combined and centrifuged as described above. A portion of the supernatant was analyzed by HPLC with a radioactivity detector (Radiomatic 150TR, Packard, Meriden, CT). A YMC-Pack ODS-A column (10 mm inner diameter (i.d.) × 150 mm, YMC, Kyoto, Japan) was used with acetonitrile/50 mM acetic acid/50 mM sodium acetate, pH 4.5 (80/10/10, v/v) at a flow rate of 2 mL/min. The retention times of [^{11}C]CB184 and [^{11}C]CB190 were 10.7 and 9.2 min, respectively. The recovery in the eluate of the injected radioactivity was essentially quantitative.

PET study

Using male Wistar rats (270–370 g), general anesthesia was induced by administering pentobarbital (50 mg/kg). After immobilizing the head using a brain stereotactic apparatus (Narishige, Tokyo, Japan), an incision was placed on the scalp to expose the skull. Using a bone drill, a hole was made in the skull to an area that was 0.4 mm anterior, 3 mm lateral, and 4.5 mm ventral to the bregma (point on the skull where the coronal and sagittal sutures converge), and solution of 6-hydroxydopamine (6-OHDA, 10 μg, Sigma-Aldrich, St. Louis, MO) in 2.5 μL physiological saline was directly injected into the right striatum [26].

Four days after the operation, the rat was anesthetized by 2 % isoflurane in O_2 (2 L/min) and placed in PET gantry of animal PET/CT system (FX-3200, Gamma Medica-Ideas, Northridge, CF) [27]. [^{11}C]CB184 or [^{11}C](*R*)-PK11195 was injected through tail vain and list-mode PET scan was carried out for 60 min. Scans by the radioligands with high and low specific radioactivity were available as we tried serial two scans from one batch of the each tracer. Injected dose is summarized in Table 5. CT data were obtained after the completion of PET acquisition. PET images were reconstructed using 3D maximum likelihood expectation maximization (MLEM) algorithm. Regions of interest (ROIs) were placed on right or left stratum with the aid of superimposed CT scull images using PMOD (PMOD Technologies, Zuerich, Switzerland). Data were expressed in standardized uptake value (SUV).

Time-activity curve (TAC) thus obtained was analyzed by indirect Logan plot method as reported by Converse [28, 29] for [^{11}C](*R*)-PK111195 employing uptake of the lesioned side as target and the contralateral side as reference. The same method was also applied to [^{11}C]CB184 in this study. The slope of the plot derives distribution volume ratio (DVR)—the ratio of distribution volume of right (6-OHDA lesioned) stratum to distribution volume of left stratum. Data were analyzed one-way ANOVA with Bonferroni's correction. Differences were considered significant at a p value less than 0.0083.

Histochemical examination

After euthanasia of the rat used in PET experiment, brain was removed and perfused for histological evaluation according to our report [10]. Numbers of tyrosine hydroxylase (TH) positive neurons were counted. Expression of mRNA coding tumor necrosis factor α (TNF-α) and interleukin-1β (IL-1β) was quantified using a RT-PCR method which was normalized by expression of NADPH [10]. Correlation between histochemistry and PET DVR was examined with Fisher's transformation which derived correlation coefficient (R) and critical value (p).

Table 2 Receptor binding affinity and partition coefficient

K_i (nM)			Log *P*	
Compound	TSPO	CBR	Calculated	Measured
CB148	0.203[a]	6880[a]	5.88[a]	2.20 ± 0.06[a]
CB184	0.537	>10000	4.99	2.06 ± 0.02[b]
CB190	0.882	>10000	3.93	2.39 ± 0.03[b]
(*R*)-PK11195	4.269[a]	7590[a]		2.54 ± 0.05[a]

[a] Data from literature [24]

[b] Mean ± SD of three runs

Results

Binding affinity octanol/water partition coefficient

Binding affinity of CB184, CB190, CB148 and (*R*)-PK11195 toward TSPO and CBR are shown in Table 2. Calculated and measured Log P values were also tabulated. Three CB compounds showed from 4.8 to 21 times higher affinity toward TSPO than (*R*)-PK11195. Selectivity of CB184 and CB190 was also higher than the other two. Especially, binding of CB184 or CB190 to CBR was under detectable range. Measured Log *P* values were similar among CB compounds, however, calculated Log *P* values were different from measured values as we previously reported [24].

Radiochemistry

Radiosynthesis of [^{11}C]CB184 and [^{11}C]CB190 could be achieved with [^{11}C]methyl triflate and acetone as reaction solvent. Decay-corrected radiochemical yield was 73 ± 12 % (n = 8) based on total [^{11}C]methyl triflate used in the synthesis and no difference between two compounds was observed. Time required for synthesis was 34 ± 2 min from the end of irradiation. The specific radioactivity was 184 ± 80 GBq/μmol (n = 8) at the end of synthesis, and the radiochemical purity was over 95 %.

Distribution of [^{11}C]CB184 and [^{11}C]CB190 in organs and brain regions

The organ distribution of radioligands was determined (Table 3) after tail vein injection of [^{11}C]CB184, [^{11}C]CB190 or [^{11}C](*R*)-PK11195. A high initial concentration of radioactivity was found in the lung, heart, and kidney. In Fig. 3, [^{11}C]CB184 and [^{11}C]CB190 showed similar time courses of regional brain distribution as [^{11}C]CB148 in the same experimental system [24]. The cerebellum and olfactory bulb showed more uptake than the other brain regions. [^{11}C](*R*)-PK11195 cleared more rapidly than three CB compounds.

Table 3 Organ distribution of radioactivity after intravenous injection of [^{11}C]CB184 and [^{11}C]CB190 into mice

Organ	Time after injection (min)				
	1	5	15	30	60
[^{11}C]CB184 uptake (%ID/g)					
Blood	5.14 ± 0.33	3.41 ± 0.56	1.51 ± 0.23	0.96 ± 0.26	0.64 ± 0.08
Heart	13.23 ± 1.44	12.34 ± 2.52	13.18 ± 5.51	13.83 ± 2.08	7.72 ± 1.69
Lung	94.82 ± 33.08	54.35 ± 15.27	25.30 ± 14.71	33.19 ± 18.49	13.82 ± 2.33
Liver	2.06 ± 3.31	9.81 ± 4.52	11.15 ± 7.75	2.69 ± 0.94	6.66 ± 1.75
Pancreas	3.66 ± 0.88	4.28 ± 1.40	5.49 ± 0.98	3.00 ± 0.87	3.57 ± 0.82
Spleen	4.12 ± 1.80	19.58 ± 6.59	13.78 ± 0.89	6.51 ± 2.13	10.08 ± 0.50
Kidney	9.04 ± 1.67	13.06 ± 2.68	42.55 ± 32.24	10.99 ± 1.93	11.69 ± 2.56
Intestine	4.47 ± 0.88	6.33 ± 2.91	3.58 ± 1.89	8.07 ± 4.84	5.08 ± 1.87
Testis	0.63 ± 0.41	1.10 ± 0.61	0.70 ± 0.30	0.58 ± 0.17	0.73 ± 0.09
[^{11}C]CB190 uptake (%ID/g)					
Blood	3.73 ± 0.83	2.42 ± 1.20	1.03 ± 0.22	0.70 ± 0.0.13	0.59 ± 0.10
Heart	15.03 ± 2.17	14.45 ± 1.85	11.74 ± 1.78	9.84 ± 1.84	10.55 ± 7.26
Lung	84.23 ± 28.14	42.18 ± 15.34	27.61 ± 6.57	19.39 ± 3.16	51.52 ± 29.19
Liver	2.65 ± 0.58	3.04 ± 0.31	5.46 ± 1.17	5.10 ± 0.77	2.09 ± 1.32
Pancreas	4.08 ± 1.23	4.40 ± 0.57	5.15 ± 0.46	4.78 ± 1.29	3.24 ± 1.74
Spleen	3.95 ± 1.39	7.59 ± 1.85	11.05 ± 2.47	11.64 ± 1.49	4.31 ± 3.12
Kidney	10.60 ± 3.43	12.92 ± 2.46	17.51 ± 0.56	15.04 ± 2.77	8.98 ± 4.94
Intestine	4.43 ± 0.55	5.47 ± 1.10	4.93 ± 1.64	3.87 ± 2.11	3.48 ± 2.59
Testis	0.86 ± 0.55	0.95 ± 0.20	1.06 ± 0.27	0.94 ± 0.15	0.62 ± 0.46

Data represent mean ± SD of four animals

Blocking studies

In vivo selectivity and specificity of [^{11}C]CB184 and [^{11}C]CB190 were examined by pretreatment with PK11195 or flumazenil. Uptake of the each radioligand in brain regions was measured at 30 min post-injection as the uptake levels were observed almost stable from 30 to 60 min post-injection. The uptake of [^{11}C]CB184 was significantly reduced relative to controls in every brain region by PK11195 (Table 4). Flumazenil had little effect on the uptake. In contrast, high uptakes of [^{11}C]CB190 in the cerebellum and olfactory bulb were significantly decreased along with PK11195 treatment, however, the other brain regions did not show the reduction. Similarly, inhibition of [^{11}C](*R*)-PK11195 uptake by cold PK11195 could not be observed in the pons and thalamus.

Metabolite studies

In HPLC analysis of plasma of mice given [^{11}C]CB184, two major radioactive peaks with the retention times of 3.5 and 5.7 min were detected except for [^{11}C]CB184 (retention time of 10.7 min). In the case of [^{11}C]CB190 (retention time 9.2 min), two major radioactive peaks were also found in the retention times of 3.5 and 5.5 min, and several minor metabolites were detected between 2.2 and 3.5 min. In the brain, the radioactive peaks in the retention times of 3.5 min were also found in addition to unchanged form of both tracers. At 30 min after injection of tracer, the percentages of the unchanged form in the brain and plasma were 92.7 ± 5.8 and 36.2 ± 15.5 %, respectively, for [^{11}C]CB184, and the corresponding figures for [^{11}C]CB190 were 86.5 ± 2.8 and 25.6 ± 7.1 %.

Animal PET studies

Time-activity curve after intravenous injection of [^{11}C](*R*)-PK11195 or [^{11}C]CB184 are shown in Fig. 4. Right and left striatum showed similar TACs when radioligands were injected in control animals (Fig. 4a, c). In contrast, 6-OHDA lesion resulted in increased uptake of both radioligands in lesioned side compared to contralateral side (Fig. 4b, d). Visual inspection revealed [^{11}C](*R*)-PK11195 was cleared more rapidly than [^{11}C]CB184. Although we tried serial two PET scans from one batch of the each tracer, the difference of pharmacological dose between low and high dose groups (Table 5) did not affect striatal uptake of both tracers (data are not shown). TACs thus obtained were analyzed by an indirect Logan plot method as reported by Converse for [^{11}C](*R*)-PK11195 employing uptake of the lesioned side as target and the contralateral side as Reference [28, 29]. Figure 5 shows satisfactory linear fitting of [^{11}C](*R*)-PK11195 or [^{11}C]CB184 in both control and lesioned animals. DVRs of [^{11}C](*R*)-PK11195

Table 4 Regional brain distribution of [^{11}C]CB184, [^{11}C]CB190 and [^{11}C](*R*)-PK11195 in mice after treatment with unlabeled drugs

Region	Injected drug		
	Control	PK11195	Flumazenil
[^{11}C]CB184 uptake (%ID/g)			
Olfactory bulb	1.45 ± 0.03	0.92 ± 0.11*	1.36 ± 0.30
Cortex	0.986 ± 0.073	0.594 ± 0.037*	0.965 ± 0.075
Striatum	0.864 ± 0.135	0.616 ± 0.026	0.806 ± 0.141
Hippocampus	1.225 ± 0.067	0.659 ± 0.099*	1.087 ± 0.122
Thalamus	0.985 ± 0.042	0.625 ± 0.024*	0.908 ± 0.159
Midbrain	0.965 ± 0.071	0.626 ± 0.031*	0.994 ± 0.228
Cerebellum	1.384 ± 0.091	0.729 ± 0.057*	1.361 ± 0.185
Pons	1.045 ± 0.102	0.655 ± 0.045*	1.003 ± 0.180
[^{11}C]CB190 uptake (%ID/g)			
Olfactory bulb	1.434 ± 0.090	1.026 ± 0.277*	1.329 ± 0.183
Cortex	0.838 ± 0.072	0.731 ± 0.227	0.722 ± 0.080
Striatum	0.715 ± 0.052	0.738 ± 0.235	0.704 ± 0.115
Hippocampus	0.887 ± 0.171	0.763 ± 0.134	0.643 ± 0.083
Thalamus	0.761 ± 0.084	0.702 ± 0.220	0.718 ± 0.097
Midbrain	0.950 ± 0.062	0.781 ± 0.214	0.830 ± 0.313
Cerebellum	1.363 ± 0.046	0.849 ± 0.232*	1.223 ± 0.275
Pons	0.890 ± 0.076	0.682 ± 0.199	0.793 ± 0.122
[^{11}C](*R*)-PK11195 uptake (%ID/g)			
Olfactory bulb	1.129 ± 0.107	0.481 ± 0.240*	1.015 ± 0.218
Cortex	0.626 ± 0.191	0.409 ± 0.112	0.606 ± 0.048
Striatum	0.507 ± 0.090	0.308 ± 0.089	0.634 ± 0.205
Hippocampus	0.730 ± 0.225	0.390 ± 0.054	0.746 ± 0.248
Thalamus	0.578 ± 0.297	0.431 ± 0.205	0.456 ± 0.068
Midbrain	0.610 ± 0.056	0.359 ± 0.052*	0.648 ± 0.134
Cerebellum	1.230 ± 0.243	0.389 ± 0.025*	1.171 ± 0.222
Pons	1.129 ± 0.107	0.481 ± 0.240	1.015 ± 0.218

Data represent mean ± SD of four animals. Blocking drugs were intravenously injected 1 min prior to the tracer administration. Data were analyzed 1-way ANOVA with Bonferroni's correction. Differences were considered significant at a p value less than 0.0167 (*)

in control and lesioned animals were 1.02 ± 0.08 ($n = 4$) and 1.15 ± 0.10 ($n = 5$), respectively, (mean ± SD). DVRs for [^{11}C]CB184 in control and lesioned animals were 1.03 ± 0.03 ($n = 4$) and 1.15 ± 0.09 ($n = 6$), respectively. Both radioligands showed significantly different DVR values between control and lesioned rats.

Correlations between the DVR values for [^{11}C](*R*)-PK11195 or [^{11}C]CB184 and histochemical data were examined. Data for both control and 6-OHDA treated rats are plotted in Fig. 6. Significant correlation ($p < 0.05$) was only seen between [^{11}C](*R*)-PK11195 and TH (Fig. 6a). Correlation between [^{11}C]CB184 and TH (Fig. 6d, $p = 0.06$) was not statistically significant, however, this would be expected with increasing number of data. The tendencies of positive correlation between DVR of [^{11}C](*R*)-PK11195 or [^{11}C]CB184 and expression of TNFα or IL-1β expression were also observed in spite they lack statistical significance (Fig. 6b, c, e, f).

Discussion

We previously reported preparation and biodistribution of four TSPO radioligands with imidazopyridineacetamide structure [24] via *N*-[^{11}C]methylation reaction. Among those, only [^{11}C]CB148 (compound **[^{11}C]7** in the previous paper) showed positive results. We are presenting herewith two another compounds of this class, [^{11}C]CB184 and [^{11}C]CB190. Radiosynthesis of these novel compounds is quite straightforward. Using [^{11}C]methyl triflate, these compounds were obtained with radiochemical yield of 73 % (decay-corrected). *O*-[^{11}C]Methylation of the phenolic hydroxyl group in the presence of small amount of NaOH should be regarded as the first choice in labeling strategy.

In vivo validation as a TSPO radioligand was firstly carried out following our previous report using normal mice [24]. In addition, an animal PET study using 6-OHDA treated rats as a model of neurodegeneration was pursued for proper estimation of feasibility of the radioligands to determine neuroinflammation process. In mice, among the brain regions examined, cerebellum and olfactory bulb showed the highest uptake of the every tracer examined. Even in normal rodents, microglia cells are present in all major divisions of brain [30]. Higher density of TSPO in the olfactory bulb of normal rodents is consistent across publications, however, TSPO density in the cerebellum should be different between animal species. In the normal rat brain cerebellar TSPO is reported to be negligible or one of the lowest among brain regions. In contrast, experiments employing mice are consistently reporting higher uptake of TSPO radioligands in cerebellum together with olfactory bulb [16, 17, 31]. In the present article [^{11}C]CB184 showed almost same performance as our previous compound [^{11}C]CB148 from regional brain distribution (Fig. 3) and from the blocking experiment (Table 3). Suppressed uptake of [^{11}C]CB190 along with pretreatment with cold PK11195 was found in limited areas in spite these two compounds share the similar TSPO binding affinity and partition coefficient. It is noteworthy that partition coefficients obtained by shaking-flask method and by CLOGP program calculation showed great difference. This situation is in accordance with our previous report [24]. At present we can not define the reason for this, however, the importance of direct measurement of partition coefficient was highlighted, again.

A rat-PET study in an injured brain model enabled more adequate expectation of feasibility of the radioligand in

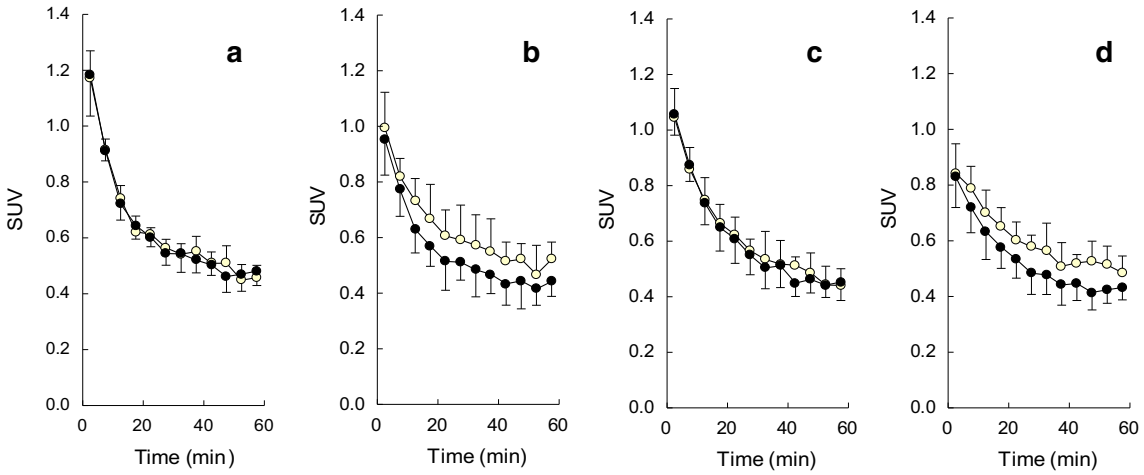

Fig. 4 Time-activity curves after i.v. injection of [^{11}C](*R*)-PK11195 or [^{11}C]CB184 to 6-OHDA lesioned rats; standardized uptake value (SUV) after intravenous injection of [^{11}C](*R*)-PK11195 (**a**, **b**) or [^{11}C]CB184 (**c**, **d**) into control (**a**, **c**) or 6-OHDA injured rat (**b**, **d**) are shown. *Open circle* shows *right* (injured) striatum and *closed circle* shows contralateral (*left*) striatum. Data are expressed as SUV (mean and SD of four animals)

Table 5 Doses of radioligands used in animal PET studies

	Radioactivity (MBq)	Pharmacological dose (nmol)		
		Total (*n*)	Low dose group (*n*)	High dose group (*n*)
[^{11}C](*R*)-PK11195	28.9 ± 6.6	2.41 ± 4.11 (9)	0.36 ± 0.28 (4)	4.45 ± 5.25 (5)
[^{11}C]CB184	29.1 ± 5.6	1.39 ± 1.96 (10)	0.19 ± 0.11 (5)	2.60 ± 2.23 (5)

Radioactivity and pharmacological dose of [^{11}C](*R*)-PK11195 and [^{11}C]CB184 were indicated. Data represent mean and SD. Number of animals was shown in the parenthesis

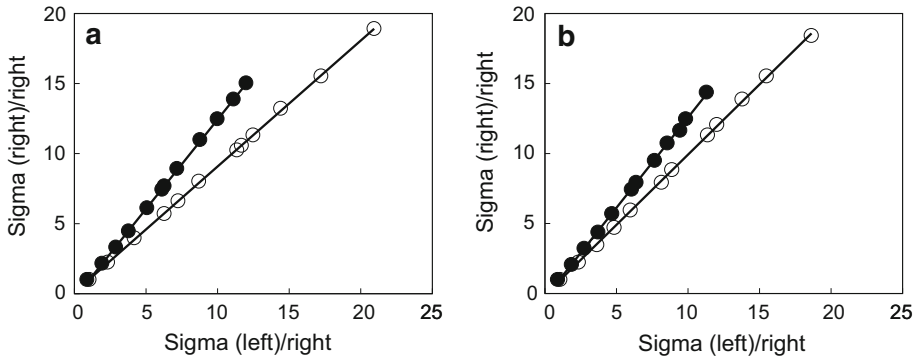

Fig. 5 Logan plot analysis; representative indirect Logan plot analysis [28, 29] of *right* and *left* striatal uptake of control (*open circle*) or 6-OHDA injured (*closed circle*) rat after intravenous injection of [^{11}C](*R*)-PK11195 (**a**) or [^{11}C]CB184 (**b**) in a rat. The analyses were carried out employing uptake of the lesioned side as target and the contralateral side as reference. After linear regression of the each plot, distribution volume ratio (DVR) between *right* and *left* striatum was obtained from its slope (see text)

patients with neurodegenerative disease. Figure 4 clearly shows that the 6-OHDA injured striatum has more uptake of TSPO tracers compared to contralateral side. Visual inspection of Fig. 4 reveals that [^{11}C]CB184 has slower washout from the rat brain than [^{11}C](R)-PK11195 due to higher binding affinity of the compound in either control or injured tissue. This tendency was in accordance with the result of mouse experiment (Fig. 3).

As TSPO is thought to exist even in normal brain tissue, the contrast between lesioned and normal brain tissue as shown in Fig. 4 does not indicate specific binding of the tracer to TSPO. It might only indicate the lesion-related

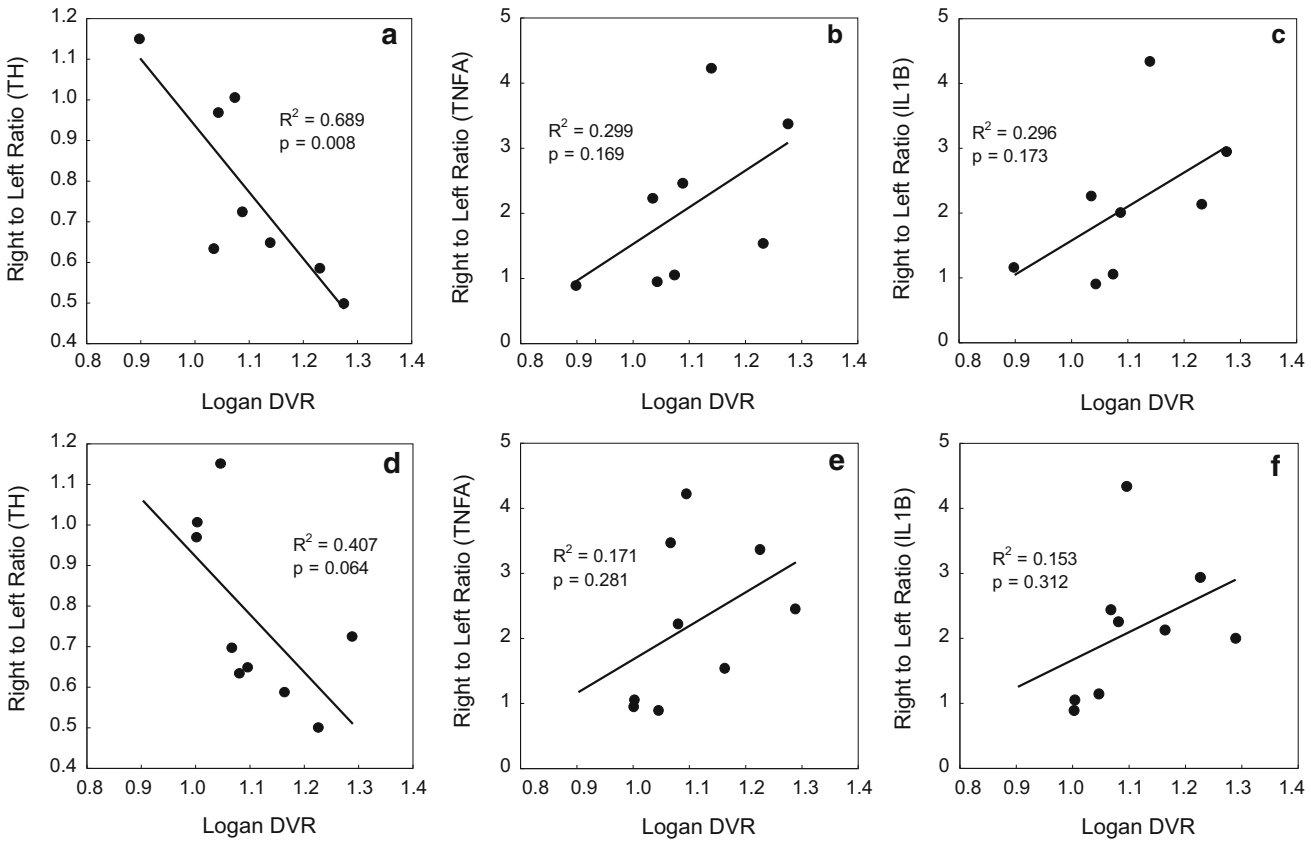

Fig. 6 Correlation between Logan DVR and *right* to *left* ratio of histochemical measures; correlation between Logan DVR and *right* to *left* ratio of number of tyrosine hydroxylase (TH) positive cell (**a**, **d**), of mRNA expression of tumor necrosis factor α (TNFA) (**b**, **e**) or interleukin-1β (IL1B) (**c**, **f**) after intravenous injection of [^{11}C](*R*)-PK11195 (**a**–**c**) or [^{11}C]CB184 (**d**–**f**) was examined. Both data from control and 6-OHDA reated rats were plotted. mRNA expression level (TNFα and IL-1β) was normalized by expression of NADPH. Data were analyzed for their correlation with Fisher's transformation. ($n = 9$ and 10 for [^{11}C]CB184 and [^{11}C](*R*)-PK11195, respectively). Regression coefficient (R^2) and critical value (p) are shown

elevation of inflammatory activity. Converse et al. [28] reported an indirect Logan plot analysis for [^{11}C](*R*)-PK11195 employing contralateral brain tissue as a reference region [29]. We also attempted this analysis and fair plot fitting and adequate DVR was obtained for both [^{11}C]CB184 and [^{11}C](*R*)-PK11195 (Fig. 5). 6-OHDA treated animals showed significantly higher DVR than non-lesioned animals for both [^{11}C]CB184 and [^{11}C](*R*)-PK11195 and the DVR shows the lesion-related elevation of inflammatory activity. DVR in 6-OHDA treated rat was 1.15 ± 0.10 for [^{11}C](*R*)-PK11195 and was 1.15 ± 0.09 for [^{11}C]CB184. These values showed no difference from ANOVA analysis and, therefore, sensitivity to detect neuroinflammation activity was similar for these two compounds.

Although we tried serial two PET scans from one batch of the each tracer, the two different pharmacological doses shown in Table 5 did not affect striatal uptake of both tracers (data not shown). As those high doses ranged from 1.3 to 6.6 nmol (from 1.6 to 7.8 μg/kg) high-end values should be regarded as maximum dose limit ensuring reproducible measurement due to low receptor occupancy. Boutin also reported that 23.7 nmol of [^{11}C](*R*)-PK11195 did not affect significantly the TACs or the contrast between the ipsilateral and contralateral side or the binding potential values [32]. Our result is in good accordance with this report.

In vivo metabolism studies showed that 36 and 25 % of radioactivity in plasma remained unchanged 30 min after intravenous injection of [^{11}C]CB184 and [^{11}C]CB190, respectively, (Table 6). It is clear contrast to the observation of [^{11}C]CB148 on which 83 % of radioactivity was observed unchanged by the same experimental system [24]. This could be explained from the difference in labeling position. As these three compounds share the *N*-dialkylacetamide substructure, a rather stable feature of [^{11}C]CB148 will explain resistance of this structure toward metabolism, however, a small amount (5 %) of polar

Table 6 Metabolite analysis

	[^{11}C]CB184		[^{11}C]CB190	
	Extraction yield (%)	Unchanged form (%)	Extraction yield (%)	Unchanged form (%)
Plasma	80.3 ± 3.3	36.2 ± 15.5	96.6 ± 3.3	25.6 ± 7.1
Brain	99.6 ± 0.1	92.7 ± 5.8	99.7 ± 0.3	86.5 ± 2.8

Data represent means and SD of three animals

metabolite was found in the brain [24]. On the other hand, polar metabolite in brain tissue was negligible for either [^{11}C]CB184 or [^{11}C]CB190.

Finally, we examined the relationship between DVR of [^{11}C](*R*)-PK11195 or [^{11}C]CB184 and histochemistry measures. We counted TH positive cells and quantified expression of inflammatory cytokines, TNFα and IL-1β mRNA by RT-PCR (Fig. 6) following our previous report [10]. We only could detect significant relationship between [^{11}C](*R*)-PK11195 DVR and left-to-right ratio of number of TH positive cells. Almost the same results were obtained when we employed right-to-left ratio of SUV value from 30 to 60 min after injection of an either radioligand (data not shown). Tight relationship between the histochemistry measures and the uptake of TSPO ligand could not be exhibited in the present examination because of limited statistical power. However, the direct comparison of PET results and inflammation indexes which can only be obtained by animal experiment will provide information concerning mechanisms underlying neurodegeneration and TSPO activation.

Recently, Yasuno et al. [33] reported that phonoxyphenyl acetamide, [^{11}C]DAA1106 binding to TSPO was significantly increased in widespread areas in subjects with mild cognitive impairment which is a prodromal state of Alzheimer's disease and this increased binding could be utilized to predict development of dementia. But a recent clinical PET study using [^{11}C]PBR28 has reported that 14 % of healthy volunteers did not have a specific binding signal in either the brain or the peripheral organs [34]. This individual difference of binding was not observed for [^{11}C](*R*)-PK11195 [35] and the similar controversy should be expected for structurally related [^{11}C]PBR06, [^{18}F]FEPPA as well as DAA family compounds. So another candidate of TSPO ligand with different structural class should be desirable also from this viewpoint.

In conclusion, we report synthesis of two carbon-11 labeled imidazopyridines TSPO ligands, [^{11}C]CB184 and [^{11}C]CB190, for PET imaging of neuroinflammation. These compounds were readily prepared by *O*-methylation reaction using [^{11}C]methyl triflate. In mice, [^{11}C]CB184 showed more uptake and specific binding than [^{11}C]CB190. In PET study using 6-OHDA treated rats, lesioned side of the brain showed higher uptake than contralateral side after i.v. injection of either [^{11}C]CB184 or [^{11}C](*R*)-PK11195. Indirect Logan plot analysis revealed distribution volume ratio (DVR) between the two sides which might indicate lesion-related elevation of TSPO binding. DVR in 6-OHDA treated mouse was 1.15 ± 0.10 for [^{11}C](*R*)-PK11195 and was 1.15 ± 0.09 for [^{11}C]CB184. These values indicate that the sensitivity to detect neuroinflammation activity was similar for these two compounds.

Acknowledgments The authors would like to thank the members of National Center for Geriatrics and Gerontology for their help. This work was supported by the Research Funding for Longevity Sciences from National Center for Geriatrics and Gerontology, Japan (21-5). All the authors disclose to have no potential conflict of interest.

References

1. Papadopoulos V, Baraldi M, Guilarte TR, Knudsen TB, Lacapère JJ, Lindemann P, et al. Translocator protein (18 kDa): new nomenclature for the peripheral-type benzodiazepine receptor based on its structure and molecular function. Trends Pharmacol Sci. 2006;27:402–9.
2. Culty M, Li H, Boujrad N, Amri H, Vidic B, Bernassau JM, et al. In vitro studies on the role of the peripheral-type benzodiazepine receptor in steroidogenesis. J Steroid Biochem Mol Biol. 1999;69:123–30.
3. Szabo I, De Pinto V, Zoratti M. The mitochondrial permeability transition pore may comprise VDAC molecules. II. The electrophysiological properties of VDAC are compatible with those of the mitochondrial megachannel. FEBS Lett. 1993;330:206–10.
4. Golani I, Weizman A, Leschiner S, Spanier I, Eckstein N, Limor R, et al. Hormonal regulation of peripheral benzodiazepine receptor binding properties is mediated by subunit interaction. Biochemistry. 2001;40:10213–22.
5. Beurdeley-Thomas A, Miccoli L, Oudard S, Dutrillaux B, Poupon MF. The peripheral benzodiazepine receptors: a review. J Neuro Oncol. 2000;46:45–56.
6. Lacapere JJ, Papadopoulos V. Peripheral-type benzodiazepine receptor: structure and function of a cholesterol-binding protein in steroid and bile acid biosynthesis. Steroids. 2003;68:569–85.
7. Banati RB. Visualizing microglia activation in vivo. Glia. 2002;40:206–17.
8. Venneti S, Lopresti B, Wiley CA. The peripheral benzodiazepine receptor in microglia: from pathology to imaging. Prog Neurobiol. 2006;80:308–22.
9. Kreutzberg GW. Microglia; a sensor for pathological events in the CNS. Trends Neurosci. 1996;19:312–8.
10. Ito F, Toyama H, Kudo G, Suzuki H, Hatano K, Ichise M, et al. Two activated stages of microglia and PET imaging of peripheral benzodiazepine receptors with [^{11}C]PK11195 in rats. Ann Nucl Med. 2010;24:163–9.
11. Shah F, Hume S, Pike V, Ashworth S, McDermott J. Synthesis of the enantiomers of [*N*-methyl-^{11}C]PK 11195 and comparison of

their behaviors as radioligands for PK binding sites in rats. Nucl Med Biol. 1994;21:573–81.
12. Belloli S, Moresco RM, Matarrese M, Biella G, Sanvito F, Simonelli P, et al. Evaluation of three quinoline carboxamide derivatives as potential radioligands for the in vivo PET imaging of neurodegeneration. Neurochem Int. 2004;44:433–40.
13. Petit-Taboué MC, Baron JC, Barré L, Travère JM, Speckel D, Camsonne R, et al. Brain kinetics and specific binding of [^{11}C]PK 11195 to omega 3 sites in baboons: positron emission tomography study. Eur J Pharmacol. 1991;200:347–51.
14. Kropholler MA, Boellaard R, Schuitemaker A, van Berckel BN, Luurtsema G, Windhorst AD, et al. Development of a tracer kinetic plasma input model for (*R*)-[11C]PK11195 brain studies. J Cereb Blood Flow Metab. 2005;25:842–51.
15. Lockhart A, Davis B, Matthews JC, Rahmoune H, Hong G, Gee A, et al. The peripheral benzodiazepine receptor ligand PK11195 binds with high affinity to the acute phase reactant alpha1-acid glycoprotein: implications for the use of the ligand as a CNS inflammatory marker. Nucl Med Biol. 2003;30:199–206.
16. Zhang M-R, Kida T, Noguchi J, Furutsuka K, Maeda J, Suhara T, et al. [^{11}C]DAA1106: radiosynthesis and in vivo binding to peripheral benzodiazepine receptors in mouse brain. Nucl Med Biol. 2003;30:513–9.
17. Zhang MR, Maeda J, Ogawa M, Noguchi J, Ito T, Yoshida Y, et al. Development of a new radioligand, *N*-(5-fluoro-2-phenoxyphenyl)-*N*-(2-[^{18}F]fluoroethoxyl-5-methoxy benzyl)acetamide, for PET imaging of peripheral benzodiazepine receptor in primate brain. J Med Chem. 2004;47:2228–35.
18. Briard E, Zoghbi S, Imaizumi M, Gourley J, Shetty U, Hong J, et al. Synthesis and evaluation of two sensitive ^{11}C-labeled aryloxyanilide ligands for imaging brain peripheral benzodiazepine receptors in vivo. J Med Chem. 2008;51:17–30.
19. Wilson A, Garcia A, Parkes H, McCormick P, Stephenson K, Houle S, et al. Radiosynthesis and initial evaluation of [^{18}F]-FEPPA for PET imaging of peripheral benzodiazipine receptors. Nucl Med Biol. 2008;35:305–14.
20. James M, Fulton R, Henderson D, Eberl S, Meikle S, Thomson S, et al. Synthesis and in vivo evaluation of a novel peripheral benzodiazepine receptor PET radioligand. Bioorg Med Chem. 2005;13:6188–94.
21. Martín A, Boisgard R, Thézé B, Van Camp N, Kuhnast B, Damont A, et al. Evaluation of the PBR/TSPO radioligand [(18)F]DPA-714 in a rat model of focal cerebral ischemia. J Cereb Blood Flow Metab. 2010;30:230–41.
22. Zhang M, Kumata K, Maeda J, Yanamoto K, Hatori A, Okada M, et al. ^{11}C-AC-5216: a novel PET ligand for peripheral benzodiazepine receptors in the primate brain. J Nucl Med. 2007;48:1853–61.
23. Mattner F, Mardon K, Katsfis A. Pharmacological evaluation of [^{123}I]-CLINDE: a radioiodinated imidazopyridine-3-acetamide for the study of peripheral benzodiazepine binding sites (PBBS). Eur J Nucl Med Mol Imaging. 2008;35:779–89.
24. Sekimata K, Hatano K, Ogawa M, Abe J, Magata Y, Biggio G, et al. Radiosynthesis and in vivo evaluation of *N*-[^{11}C]methylated imidazopyridineacetamides as PET tracers for peripheral benzodiazepine receptors. Nucl Med Biol. 2008;35:327–34.
25. Denora N, Laquintana V, Pisu MG, Dore R, Murru L, Latrofa A, Trapani G, Sanna E. 2-Phenyl-imidazo[1,2-a]pyridine compounds containing hydrophilic groups as potent and selective ligands for peripheral benzodiazepine receptors: synthesis, binding affinity and electrophysiological studies. J Med Chem. 2008;2008(51):6876–87.
26. Toyama H, Hatano K, Suzuki H, Ichise M, Momosaki S, Kudo G, et al. In vivo imaging of microglial activation using a peripheral benzodiazepine receptor ligand: [^{11}C]PK-11195 and animal PET following ethanol injury in rat striatum. Ann Nucl Med. 2008;22:417–24.
27. Bergeron M, Cadorette J, Beaudoin JF, Lepage MD, Robert G, Selivanov V, et al. Performance evaluation of the LabPET APD-based digital PET scanner. IEEE Trans Nulc Sci. 2009;56:10–6.
28. Converse AK, Larsen EC, Engle JW, Barnhart TE, Nickles RJ, Duncan ID. ^{11}C-(R)-PK11195 PET imaging of microglial activation and response to minocycline in Zymosan-treated rats. J Nucl Med. 2011;52:257–62.
29. Logan J, Fowler JS, Volkow ND, Wang GJ, Ding YS, Alexoff DL. Distribution volume ratios without blood sampling from graphical analysis of PET data. J Cereb Blood Flow Metab. 1996;16:834–40.
30. Lawson LJ, Perry VH, Dri P, Gordon S. Heterogeneity in the distribution and morphology of microglia in the normal adult mouse brain. Neurosci. 1990;39:151–70.
31. Chen MK, Baidoo K, Verina T, Guilarte TR. Peripheral benzodiazepine receptor imaging in CNS demyelination: functional implications of anatomical and cellular localization. Brain. 2004;127:1379–92.
32. Boutin H, Chauveau F, Thominiaux C, Gregoire MC, James ML, Trebossen R, Hantraye P, Dolle F, Tavitian B, Kassiou M. ^{11}C-DPA-713: a novel peripheral benzodiazepine receptor PET ligand for in vivo imaging of neuroinflammation. J Nucl Med. 2007;48:573–81.
33. Yasuno F, Kosaka J, Ota M, Higuchi M, Ito H, Fujimura Y, Nozaki S, Takahashi S, Mizukami K, Asada T, Suhara T. Increased binding of peripheral benzodiazepine receptor in mild cognitive impairment-dementia converters measured by positron emission tomography with [(11)C]DAA1106. Psychiatry Res. 2012;203:67–74.
34. Fujita M, Imaizumi M, Zoghbi SS, Fujimura Y, Farris AG, Suhara T, Hong J, Pike VW, Innis RB. Kinetic analysis in healthy humans of a novel positron emission tomography radioligand to image the peripheral benzodiazepine receptor, a potential biomarker for inflammation. Neuroimage. 2008;40:43–52.
35. Owen DR, Howell OW, Tang SP, Wells LA, Bennacef I, Bergstrom M, Gunn RN, Rabiner EA, Wilkins MR, Reynolds R, Matthews PM, Parker CA. Two binding sites for [^{3}H]PBR28 in human brain: implications for TSPO PET imaging of neuroinflammation. J Cereb Blood Flow Metab. 2010;30(9):1608–18.